Dalton Transactions

RSC Publishing

PAPER

View Article Online
View Journal | View Issue

Cite this: *Dalton Trans.*, 2013, **42**, 9157

Organometallic mediated radical polymerization of vinyl acetate using bis(imino)pyridine vanadium trichloride complexes†‡

Mitchell R. Perry,[a] Laura E. N. Allan,[a,b] Andreas Decken[c] and Michael P. Shaver*[a,b]

Received 2nd November 2012,
Accepted 9th January 2013

DOI: 10.1039/c3dt32625j

www.rsc.org/dalton

The synthesis and characterization of one novel proligand and six novel vanadium(III) trichloride complexes is described. The controlled radical polymerization activity towards vinyl acetate of these, and eight other bis(imino)pyridine vanadium trichloride complexes previously reported, is investigated. Those complexes possessing variation at the *N*-aryl *para*-position with no steric protection offered by *ortho*-substituents (4 examples) result in poor control over poly(vinyl acetate) polymerization. Control is improved with increasing steric bulk at the *ortho*-position of the *N*-aryl substituent (4 examples) although attempts to increase steric bulk past isopropyl were unsuccessful. Synthesizing bis(imino)pyridine vanadium trichloride complexes with substituted imine backbones restores polymerization control when aliphatic substituents are used (4 examples) but ceases to make any drastic improvements on catalyst lifetime. Modification of the polymerization conditions is also investigated, in an attempt to improve the catalyst lifetime. Expansion of the monomer scope to include other vinyl esters, particularly those derived from renewable resources, shows promising results.

Introduction

The importance of controlled radical polymerization (CRP) is growing as the demand for specific polymer architectures with controlled properties increases.[1–3] While several techniques to realize this goal have been developed,[3–6] the central tenet of CRP aims to minimize the concentration of propagating radicals at any one time. This is achieved by establishing equilibrium (k_a/k_d, where k_a is the activation rate constant and k_d is the deactivation rate constant) between a dormant, 'capped' species and an active species capable of propagation (Scheme 1), thereby decreasing undesirable side reactions including radical combination and disproportionation.[7] Atom transfer radical polymerization (ATRP) is probably the most researched metal-mediated CRP technique and utilizes a halogen spin-trap to generate polymers reversibly terminated with carbon–halogen bonds.[8–13]

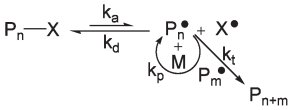

Scheme 1 Activation and deactivation processes in CRP reactions.

Much recent research interest has focused on organometallic mediated radical polymerization (OMRP),[1–3,13–16] which uses an organometallic species as the radical trap to impart control over the polymerization. Cobalt systems are the most prolific in OMRP, with $Co(acac)_2$ capable of controlling the polymerization of several monomer families including acrylates,[17–19] acrylonitrile[20–23] and vinyl acetate (VAc),[24–29] a notoriously difficult monomer to control due to the difficulty in both activating this monomer and controlling the equilibrium between the unstabilized radical and the dormant species. A long induction period and the use of an inconvenient initiator, V-70, which requires storage at low temperatures, are negatives of this system. The induction period can be circumvented with PVAc-$Co(acac)_2$ macroinitiators, however, laborious synthesis and purification hinder commercialization of this methodology.[28,29] Other alternatives to decrease this initiation period include utilizing a redox system comprising the sodium salt of citric acid and lauroyl or benzoyl peroxide, capable of generating vinyl ester polymers with PDIs as low as

[a]*University of Prince Edward Island, 550 University Avenue, C1A 4P3 Charlottetown, PE, Canada*
[b]*School of Chemistry, University of Edinburgh, Joseph Black Building, West Mains Road, Edinburgh, EH9 3JJ, UK. E-mail: michael.shaver@ed.ac.uk; Fax: +44 (0) 131650 4743; Tel: +44 (0) 131 650 4726*
[c]*University of New Brunswick, P.O. Box 4400, E3B 6E2 Fredericton, NB, Canada*
†Celebrating 300 years of Chemistry at Edinburgh.
‡Electronic supplementary information (ESI) available: Additional polymerization data, X-ray crystallography data, GPC traces. CCDC 891100 and 891101. For ESI and crystallographic data in CIF or other electronic format see DOI: 10.1039/c3dt32625j

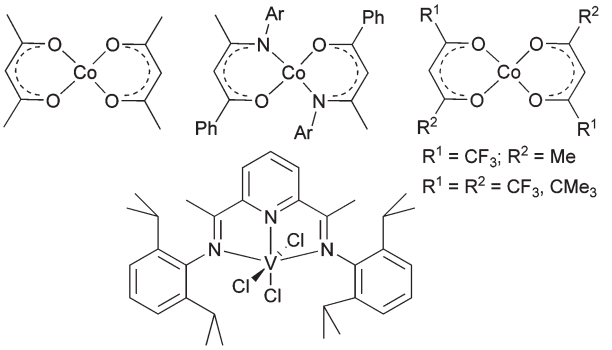

Fig. 1 Efficient mediators of vinyl acetate OMRP.

1.2.[30,31] Modification of this versatile cobalt system to include fluorinated acac substituents,[17,32] the more electron-donating tetramethylheptadionato ligands,[33] as well as isoelectronic β-ketoiminate ligands[34] (Fig. 1) have expanded the scope of complexes to show efficacy in vinyl acetate OMRP. However, aside from cobalt systems, there remains a paucity of metal systems capable of efficiently controlling the polymerization of VAc through OMRP or other CRP techniques.

Bis(imino)pyridine [BIMPY] complexes, where [BIMPY] = 2,6-(ArN=CMe)$_2$C$_5$H$_3$N, with a variety of metals have been developed previously for ethylene polymerization, as documented in a comprehensive review by Gibson *et al.*[35] and other noteworthy literature reports.[36–46] Vanadium [BIMPY] complexes are active in olefin polymerization,[38–40,47–50] and our group has recently shown its promise in OMRP.[51,52] Using a vanadium(III) [BIMPY] system (Fig. 1), where Ar = 2,6-^{i}Pr$_2$C$_6$H$_3$ ([BIMPY]^{dipp}VCl$_3$), **1**, with azobisisobutyronitrile (AIBN) as the initiator, controlled poly(vinyl acetate) (PVAc) can be synthesized with excellent agreement between theoretical and experimental molecular weights and narrow PDIs (<1.3). Control is maintained for approximately 3 hours at 120 °C, after which time molecular weights deviate from theoretical values and productive polymerization ceases.[51,52] This report details the synthetic investigation of structurally similar vanadium(III) complexes for the OMRP of vinyl acetate, to further investigate this loss of control. Attention is also paid to expansion of the monomer scope of [BIMPY]^{dipp}VCl$_3$ to include other vinyl ester monomers and optimization of the polymerization conditions.

Results and discussion

Synthesis of vanadium(III) complexes

A variety of proligands were synthesized from the imine condensation between the appropriate ketone or aldehyde and the relevant amine. From these proligands, a family of structurally similar [BIMPY]VCl$_3$ complexes were obtained, following a previously reported procedure.[52] Complexes with substituents varying in electronic character and steric bulk at the *para*- and *ortho*-positions of the *N*-aryl substituent and at the imine carbon backbone positions were synthesized (Scheme 2).

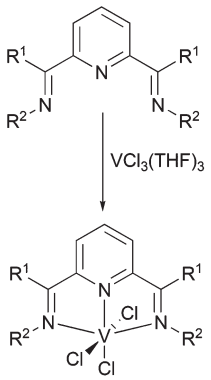

	R^1	R^2
1	Me	2,6-^{i}Pr$_2$C$_6$H$_3$
2	Me	Ph
3	Me	4-MeC$_6$H$_4$
4	Me	4-MeOC$_6$H$_4$
5	Me	4-FC$_6$H$_4$
6	Me	2,6-Me$_2$C$_6$H$_3$
7	Me	2,6-Et$_2$C$_6$H$_3$
8	Me	2,4,6-Me$_3$C$_6$H$_2$
9	Me	Cy
10	H	2,6-^{i}Pr$_2$C$_6$H$_3$
11	Ph	2,6-^{i}Pr$_2$C$_6$H$_3$
12	Et	2,6-^{i}Pr$_2$C$_6$H$_3$
13	^{i}Pr	2,6-^{i}Pr$_2$C$_6$H$_3$
14	Ph	Ph

Scheme 2 Synthesis of substituted [BIMPY]VCl$_3$ complexes.

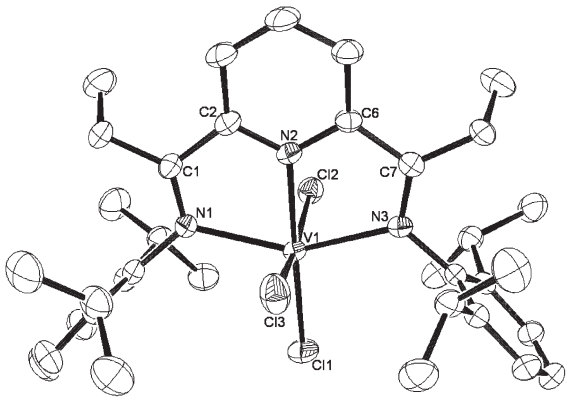

Fig. 2 X-ray crystal structure of **12**, with hydrogen atoms removed for clarity and ellipsoids shown at the 50% probability level.

Crystals suitable for X-ray crystallography were obtained for novel complexes **12** and **14** from the slow evaporation of dilute acetonitrile solutions. In the X-ray crystal structure of **12** the vanadium centre lies in a distorted octahedral geometry with an equatorial plane defined by the three nitrogen atoms of the [BIMPY] ligand [N(3)–V(1)–N(2) = 75.38(8)°, N(2)–V(1)–N(1) = 75.52(8)°, N(1)–V(1)–N(3) = 150.72(8)°] and one chlorine atom [N(3)–V(1)–Cl(1) = 103.67(6)°, N(1)–V(1)–Cl(1) = 105.57(6)°, N(2)–V(1)–Cl(1) = 176.42(6)°] (Fig. 2). The remaining chlorine atoms (Cl(2) and Cl(3)) form a bent axial vector [Cl(2)–V(1)–Cl(3) = 168.36(3)°], albeit with a large deviation from 180°, potentially due to the increased steric repulsion present in this system. Imine bond distances [C(7)–N(3) = 1.292(3) Å, C(1)–N(1) = 1.280(3) Å] are in good agreement with similar structures in the literature.[53] V–N(pyridine) π-bonding is suggested by the shorter vanadium–nitrogen bond distance present between the metal centre and the pyridine nitrogen [V(1)–N(2) = 2.063(2) Å] *versus* the vanadium–nitrogen bonds to imino nitrogen atoms [V(1)–N(3) = 2.188(2) Å and V(1)–N(1) = 2.213(2) Å]. Selected bond lengths and angles are summarized in Table 1.

The equatorial plane defined by the three nitrogen atoms of the [BIMPY] ligand [N(3)–V(1)–N(2) = 74.58(17)°, N(2)–V(1)–N(1) = 74.98(17)°, N(1)–V(1)–N(3) = 149.38(16)°] and one

Table 1 Selected geometrical parameters for complexes **12** and **14**

Bond distances (Å) and angles (°)			
Complex **12**		Complex **14**	
V(1)–Cl(1)	2.2918(13)	V(1)–Cl(1)	2.3033(15)
V(1)–Cl(2)	2.3339(11)	V(1)–Cl(2)	2.3393(16)
V(1)–Cl(3)	2.2862(12)	V(1)–Cl(3)	2.3181(17)
V(1)–N(1)	2.213(2)	V(1)–N(1)	2.153(4)
V(1)–N(2)	2.063(2)	V(1)–N(2)	2.074(4)
V(1)–N(3)	2.188(2)	V(1)–N(3)	2.155(4)
N(1)–C(1)	1.280(3)	N(1)–C(1)	1.305(6)
N(3)–C(7)	1.292(3)	N(3)–C(7)	1.301(6)
N(1)–V(1)–N(2)	75.52(8)	N(1)–V(1)–N(2)	74.98(17)
N(2)–V(1)–N(3)	75.38(8)	N(2)–V(1)–N(3)	74.58(17)
N(1)–V(1)–N(3)	150.72(8)	N(1)–V(1)–N(3)	149.38(16)
N(1)–V(1)–Cl(1)	105.57(6)	N(1)–V(1)–Cl(1)	104.81(12)
N(3)–V(1)–Cl(1)	103.67(6)	N(3)–V(1)–Cl(1)	105.75(12)
N(2)–V(1)–Cl(1)	176.42(6)	N(2)–V(1)–Cl(1)	177.40(14)
Cl(2)–V(1)–Cl(3)	168.36(3)	Cl(2)–V(1)–Cl(3)	173.30(7)

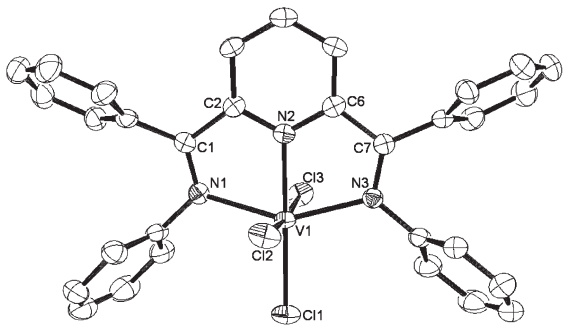

Fig. 3 X-ray crystal structure of **14**, with hydrogen atoms removed for clarity and ellipsoids shown at the 50% probability level.

chlorine atom [N(3)–V(1)–Cl(1) = 105.75(12)°, N(1)–V(1)–Cl(1) = 104.81(12)°, N(2)–V(1)–Cl(1) = 177.40(14)°] that makes up the distorted octahedral geometry of **14** is comparable to that of **12** (Fig. 3). The axial vector defined by the vanadium–chlorine bonds [Cl(2)–V(1)–Cl(3) = 173.30(7)°] is expectedly less bent than those in the crystal structure of **12**, as **14** possesses no steric repulsion from aryl *ortho* substituents. With the decreased steric bulk at the 2,6-aryl positions, there is a significant increase in the Cl(2)–V(1)–Cl(3) bond angles. It is also evident that the equatorial vanadium–chlorine bonds present in **14** [V(1)–Cl(1) = 2.3033(15) Å, V(1)–Cl(2) = 2.3393(16) Å] are consistently longer than those found in **12**. Furthermore, imine bond distances [C(7)–N(3) = 1.301(6) Å, C(1)–N(1) = 1.305(6) Å] are noticeably longer than those of **12** and other complexes possessing alkyl-substituted imine carbons,[53] suggesting a weaker imine bond and a more electrophilic imine carbon.

Vinyl acetate polymerization data

Variation of the *para*-substituent at the *N*-aryl (R^2) position (Scheme 2, complexes **2–5**) resulted in interesting polymerization activity towards VAc (Table 2). Although reasonable agreement between experimental and theoretical molecular weights

Table 2 Polymerization data for **1–9**[a]

Complex	% Conversion[b]	M_n[c]	$M_{n,th}$[d]	PDI
1	26	2830	4520	1.3
2	44	8330	6350	1.8
3	30	5440	4310	1.6
4	29	7590	4300	1.8
5	42	159 210	3030	1.4
		4350		1.4
5[e]	22	3190	3150	1.4
6	48	10 270	8180	2.1
7	41	7310	5230	1.7
8	48	10 000	7300	2.1
9	65	11 010	9310	2.7

[a] Reactions carried out in bulk at 120 °C for 3 h using AIBN and monomer : catalyst : initiator ratios of 100 : 1 : 0.6. [b] Determined gravimetrically. [c] M_n obtained using polystyrene standards and corrected for VAc. [d] $M_{n,th} = [M]_0/[I]_0 \times MW(monomer) \times \%\ conv. + MW(catalyst)$. [e] Polymerization run with monomer : catalyst : initiator ratio of 100 : 0.6 : 3.

is observed, control is poor as indicated by the relatively broad PDIs (1.4–1.8). Interestingly, the presence of an electron-withdrawing *para*-fluoro substituent in the complex, **5**, generates polymers with bimodal GPC traces (Fig. S1, ESI‡). The expected signal for a polymer of molecular weight *ca.* 4000 Da is complicated by a further, high molecular weight peak at *ca.* 159 000 Da, resulting from rapid, uncontrolled polymerization. Increasing the concentration of complex in the polymerization reaction circumvents this problem as more radical trap is present in the system to deactivate the propagating chains, resulting in consistently monomodal GPC traces. However, polymerizations were still less controlled than those utilizing the parent complex, $[BIMPY]^{dipp}VCl_3$, **1**.

Polymerization results obtained using complexes **2–5** suggest that the *N*-aryl *para*-substituents are not the predominant determining factor with respect to imparting control in the polymerization of vinyl acetate. We felt that the loss of control was likely due to the removal of steric bulk from the *ortho* positions. Therefore, a series of complexes varying in *N*-aryl *ortho*-substitution, **6–8**, were screened. Complex **6**, possessing 2,6-dimethyl substituents resulted in poorly controlled polymerization reactions, with PDIs of 2.1. However, when increasing the steric bulk from methyl, **6**, to ethyl, **7**, a significant decrease in the PDI to 1.7 is observed. Furthermore, when moving to isopropyl *ortho*-substituents, **1**, a further decrease in PDI, to 1.3, is observed. This strongly supports the suggestion that increased steric bulk at the *ortho*-positions of the aryl ring increases the OMRP control which these $[BIMPY]VCl_3$ complexes exert over vinyl acetate. Attempts to increase this bulk further are ongoing but have so far been unsuccessful, due to unfavourable condensation reactions. A comparison of data obtained for **6** and **8**, which differ only in the presence of a methyl group at the *para*-position illustrates the lack of importance of the *para*-substituent: both complexes reach 48% conversion in 3 h, with PDIs of 2.1, indicating that *para*-substitution does not play a significant role in tuning the polymerization behaviour of these vanadium complexes.

Interestingly, screening complex **9** (Table 2), possessing an aliphatic cyclohexyl *N*-substituent, led to relatively high conversion (65%) and a large increase in PDI (2.7). It is likely that the disruption in conjugation throughout the ligand backbone is responsible for loss of the ligand non-innocence.[52] The relatively high conversions and high PDIs support a metal centre that is more electron-rich and less likely to form a bond with propagating radicals, resulting in poor deactivation and an uncontrolled polymerization.

The results presented in Table 2 suggest that steric bulk is necessary at the *ortho*-positions to impart control over the polymerization of the reactive vinyl acetate monomer. It is likely that increased steric bulk may offer protection from attack by incoming radicals, a theory supported by our computational investigation.[52] To further probe the system, a 2-methylpyridyl alkylated $[BIMPY]^{dipp}V(III)$ compound was synthesized using the method of Gambarotta *et al*.[53] This structurally similar compound lacks the conjugation responsible for ligand non-innocence in the $[BIMPY]VCl_3$ complexes and is suggestive of products arising from radical attack at the ligand backbone. Screening this V(III) complex for the polymerization of VAc resulted in no polymer, supporting alkylation *via* radical attack on the ligand framework acting as a deactivation mechanism.

One way to mitigate the occurrence of this radical attack is to protect the face of the ligand by increasing steric bulk at the imine carbon position (R^1). A family of $[BIMPY]VCl_3$ catalysts with different substituents at the imine carbon were synthesized, **10–14**, with their VAc OMRP screening results summarized in Table 3.

As expected, complex **10**, with no steric protection at the imine carbon position, exhibits low polymerization activity generating only short oligomers that could not be accurately characterized by GPC. Similar data are obtained after conducting the polymerization for 5 hours. Complex **11**, with a phenyl imine substituent, gives relatively high conversions (50%) after 3 hours, but displays poor control as indicated by the broad PDI of 2.0. The presence of aromatic substituents on the backbone potentially disrupts the ligand non-innocence and the OMRP equilibrium. The planar phenyl group does appear to offer some steric protection; however, the electron-withdrawing character of this substituent soon trumps the increased steric bulk by creating a more electrophilic imine carbon, susceptible to radical attack. Conversions did not increase above 50% despite reaction times as long as 5 hours.

The effect of increasing steric bulk on the backbone imine carbon can be best observed in the series of complexes with 2,6-diisopropyl phenyl *N*-aryl substituents and varying R^1 substituents. As bulk is increased from methyl, **1**, to ethyl, **12**, to isopropyl, **13**, control over the polymerization is maintained, with PDIs of 1.2–1.3 and excellent correlation between experimental and theoretical molecular weights. Higher molecular weight polymers were targeted using **12**, running the reactions with an increased concentration of monomer (1 : 200 : 0.6 and 1 : 500 : 0.6). Control was slightly decreased, with PDIs of 1.3–1.4, and increased molecular weights of 3570 and 6680, respectively. Conversions decreased to 12.5% in both cases. This slight decrease in control is attributed to the increased concentration of monomer in the system, which leads to a larger number of uncontrolled monomer insertions before the propagating species becomes dormant, thereby increasing PDIs.

The absence of *N*-aryl *ortho* substituents in complex **14**, which has phenyl substituents at both the imine carbon and *N*-aryl positions, resulted in low conversions, independent of reaction time. Interestingly, in contrast to **11**, which has 2,6-diisopropyl phenyl substituents at the *N*-aryl position and phenyl substituents at the imine carbon, excellent control was achieved, with molecular weights in good agreement with theoretical values and low PDIs of 1.3, albeit at low conversions (16%). This is indicative of radical attack occurring early due to lack of protection from *ortho*-substituents.

Reaction optimization

Optimization of vinyl acetate polymerization was carried out using the parent $[BIMPY]^{dipp}VCl_3$ complex, **1**, since it remains one of the most efficient OMRP mediators in this family of bis(imino)pyridine complexes, **1–14**.

The use of higher initiator concentrations results in increased conversions, from 26% when 0.6 equivalents of AIBN are used to 46% with 6 equivalents of AIBN (Table 4). Molecular weights decrease somewhat (*ca*. 1000 Da for the 10-fold increase in [AIBN]), but not as much as might be expected for these elevated radical concentrations. PDIs are largely unaffected, remaining at *ca*. 1.3 even when 6 equivalents of AIBN are used, indicating that the radical exchange is rapid and trapping of the propagating chains by the vanadium complex is efficient. However, extending reaction times to 6 hours does not result in higher conversions at any of the

Table 3 Polymerization data for **10–14**[a]

Complex	% Conv.	M_n	$M_{n,th}$	PDI
10	15	—	—	—
11	50	9270	7230	2.0
12	22	2480	2360	1.2
13	25	3060	3450	1.3
14	16	2400	2180	1.3

[a] Reaction and characterization details as provided in Table 2.

Table 4 Effect of AIBN concentration on VAc polymerization using **1**[a]

AIBN equiv.	% Conv.	M_n	PDI
0.6	28	4820	1.3
1.2	31	2430	1.3
6	47	1710	1.3

[a] Reactions carried out in bulk at 120 °C for 3 h using AIBN and monomer : catalyst ratios of 100 : 1 with other parameters as in Table 2.

Table 5 Effect of temperature on VAc polymerization using **1**[a]

Temp. (°C)	% Conv.	M_n	$M_{n,th}$	PDI
120	28	4820	3830	1.3
110	23	4070	3390	1.3
100	25	4370	4230	1.4
90	29	4970	4770	1.4

[a] Reactions carried out in bulk at variable temperatures for 3 h with other reaction and characterization parameters as in Table 2.

Table 6 Effect of temperature on VAc polymerization using V-65 and **1**[a]

Temp. (°C)	% Conv.	M_n	$M_{n,th}$	PDI
110	27	4580	5620	1.4
100	25	4290	5420	1.4
90	23	4000	5410	1.4
80	29	4880	7170	1.4
70	36	5900	7940	1.5

[a] Reactions carried out in bulk for 6 h using V-65 with other reaction and characterization parameters as in Table 2.

radical concentrations investigated (Table S2, ESI‡), indicating that catalyst death occurs irrespective of radical concentration.

We then investigated the effects of temperature on the polymerization behaviour of our system. Decreasing the temperature of the polymerization from 120–90 °C has little effect on VAc conversions, which are between 23–29% (Table 5). As expected, PDIs are broader at the lower temperatures, as a result of less efficient AIBN initiation at these temperatures and slower radical exchange between propagating and dormant species. After 6 hours, the catalyst is essentially inactive as no increase in conversion is observed when running the polymerizations for 24 hours (Table S3, ESI‡).

We also explored the efficacy of **1** using another radical initiator, V-65, which has a lower 10 hour half-life decomposition temperature than AIBN. Although lower temperatures using V-65 favour higher conversions (Table 6), which decrease from 36% at 70 °C to 27% at 110 °C, the PDIs increase significantly from 1.36 (at 110 °C) to 1.51 (at 70 °C) as the temperature is decreased. This implies that radical exchange is less efficient at these lower temperatures, which results in the increased PDIs but also in a slower rate of catalyst death, meaning that conversions are also increased. Molecular weights are slightly higher than theoretical values, with greater deviation at the lower temperatures. Catalyst death is still significant, as illustrated by the conversions at 24 h (Table S4, ESI‡), which are almost identical to those obtained at 6 h.

Expansion of the monomer scope

$[BIMPY]^{dipp}VCl_3$, **1**, has previously shown some efficacy in the polymerization of vinyl propionate (VPr), vinyl pivalate (VPv) and vinyl benzoate (VBz).[52] While control over VPr and VPv is reasonable, with PDIs of ≤1.4, polymerization of VBz yields polymers with broadened PDIs of 1.5–1.6 (Table 7). No productive polymerization occurs after 6 hours, with conversions,

Table 7 Polymerization data for vinyl ester monomers using **1**[a]

Monomer	Time/h	% Conv.[b]	M_n[c]	$M_{n,th}$[d]	PDI
VPr	6	20	3530	3990	1.3
VPr	24	18	3570	3660	1.4
VPv	6	36	9340	8320	1.4
VPv	24	30	10 550	7040	1.4
VBz	6	20	3960	5620	1.6
VBz	24	19	3280	5370	1.5
VLa	1	10	8760	3700	1.5
VLa	6	16	8380	6070	1.5
VLa	64	16	9040	5390	1.6
VLa[e]	6	7	4460	2440	1.4
VSt	1	24	11 060	3670	1.5
VSt	3	27	9930	4160	1.5
VSt	6	51	12 540	5470	1.7

[a] Reactions carried out in bulk at 120 °C using AIBN and ratios of 100 : 1 : 0.6 for monomer : catalyst : initiator. [b] Determined by ^{1}H NMR spectroscopy. [c] M_n corrected for VAc. [d] $M_{n,th} = [M]_0/[I]_0 \times$ MW (monomer) × %conversion + MW(catalyst). [e] Reaction conducted in 1 mL toluene.

molecular weights and PDIs largely unaffected by longer reaction times. Some deviations between observed and theoretical molecular weights are to be expected, as the experimental molecular weights were corrected using the vinyl acetate conversion factor which will not account for the differences in hydrodynamic volumes between these vinyl ester polymers and poly(vinyl acetate).

As observed for poly(vinyl acetate), decreasing the temperature of the polymerization from 120–90 °C has little effect on prolonging the catalyst lifetime. Similar trends to those described for vinyl acetate are observed with vinyl propionate, vinyl pivalate and vinyl benzoate (Tables S5–S7, ESI‡) although conversions are somewhat improved at lower temperatures for both vinyl propionate and vinyl pivalate. PDIs again tend to be broader at these lower temperatures, while the molecular weights increase as higher conversions are reached.

The study of vinyl esters was further extended to include long chain vinyl monomers of fatty acids. In particular, vinyl laurate (VLa) and vinyl stearate (VSt) were chosen due to their commercial availability and scarcity of reports focusing on control over these renewable monomers. One very recent literature report utilizes $Co(acac)_2$ to generate homopolymers and block co-polymers of VLa and VSt with good control (PDI < 1.3), using a redox initiator.[54] Conversions for the screening reactions of VLa using **1** were limited to 16% conversion at 120 °C, initiated by AIBN, despite reaction times as long as 64 h (Table 7). Control is modest when the polymerizations are carried out in bulk, with broadened PDIs of 1.5–1.6. Running the polymerizations in solution offers improved control and PDIs of 1.4, but a concomitant decrease in conversion is observed, as the likelihood of radical combination increases. Increased conversions are observed with VSt, as the inherent viscosity of the molten monomer hinders termination, a property of the decreased rates of diffusion present in the reaction.[55] It should also be noted that larger deviations between theoretical and experimental molecular weights are observed

for these monomers and are attributed to the different hydrodynamic volumes of the respective polymers, as the data in Table 7 are corrected for VAc.

Conclusions

We report the synthesis of several new vanadium trichloride complexes based on bis(imino)pyridyl ligand frameworks. A family of structurally similar complexes were screened for their polymerization activity towards VAc in bulk. Substituents at the *N*-aryl *para*-position (**2–5**) have less impact than the *ortho*-substituents (**1**, **6–8**) on imparting control over the polymerization. Increasing the steric bulk at the *ortho*-positions of the *N*-aryl substituent increases control over the polymerization, with isopropyl substituents giving the best results. Furthermore, substitution at the imine carbon also significantly affects polymerization behaviour. No steric bulk, **10**, hinders polymerization early, as does the presence of a phenyl group on the backbone, **11**, although this effect can be somewhat mitigated by removing *ortho*-substitution at the *N*-aryl positions, **14**. Alkylating the imine carbon substituents restores control over the polymerization (**1**, **12**, **13**), but has so far been ineffective at significantly increasing the lifetime of these OMRP catalysts. Attempts to further increase steric bulk at the *N*-aryl *ortho*-positions are ongoing. Use of *N*-alkyl substituents interrupts the delocalization within the ligand framework and results in inferior OMRP behaviour (**9**).

The efficacy of **1** with respect to other monomers and initiators was also explored, with modest control observed for vinyl laurate, vinyl stearate and vinyl benzoate. Improved control over vinyl propionate and vinyl pivalate was observed, although catalyst lifetimes were not significantly improved for any monomer by lowering the reaction temperatures, changing initiators or by increasing the concentration of initiator.

Experimental

General considerations

All chemistry with air/moisture sensitive compounds was conducted under nitrogen using standard Schlenk and cannula techniques or performed in an MBraun LABmaster sp glovebox equipped with a −35 °C freezer, [O_2] and [H_2O] analyzers. Elemental analyses were performed at Guelph Chemical Laboratories Ltd. NMR spectroscopy was performed on a Bruker Avance 300 MHz spectrometer, operating at 300 and 75 MHz for ^{1}H and ^{13}C nuclei respectively, at 293 K unless otherwise stated. *J* values are given in Hz. All ^{13}C NMR spectra reported are proton decoupled and calibrated relative to the residual proton signals in the deuterated solvent. All paramagnetic ^{1}H NMR spectroscopy signals are reported as singlets, unless otherwise stated. Infra-red spectra were obtained either as nujol mulls or as solids using transmittance or ATR (Attenuated Total Reflectance), respectively, on a Bruker Alpha spectrometer, with listed absorbances corresponding to imine stretches. DCM and MeCN and liquid monomers were dried over CaH_2, trap-to-trap distilled and degassed in three freeze–pump–thaw cycles prior to use. All solvents were degassed prior to use.

Ligands synthesized according to literature procedures are listed here: **L1** (R^1 = Me, R^2 = 2,6-^{i}Pr$_2$C$_6$H$_3$),[36] **L2** (R^1 = Me, R^2 = Ph),[56] **L3** (R^1 = Me, R^2 = 4-MeC$_6$H$_4$),[37] **L4** (R^1 = Me, R^2 = 4-MeOC$_6$H$_4$),[37] **L5** (R^1 = Me, R^2 = 4-FC$_6$H$_4$),[44] **L6** (R^1 = Me, R^2 = 2,6-Me$_2$C$_6$H$_3$),[36] **L7** (R^1 = Me, R^2 = 2,6-Et$_2$C$_6$H$_3$),[57] **L8** (R^1 = Me, R^2 = 2,4,6-Me$_3$C$_6$H$_2$),[36] **L9** (R^1 = Me, R^2 = C$_6$H$_{11}$, Cy),[57] **L10** (R^1 = H, R^2 = 2,6-^{i}Pr$_2$C$_6$H$_3$),[36] **L11** (R^1 = Ph, R^2 = 2,6-^{i}Pr$_2$C$_6$H$_3$),[58] **L12** (R^1 = Et, R^2 = 2,6-^{i}Pr$_2$C$_6$H$_3$),[43] **L13** (R^1 = ^{i}Pr, R^2 = 2,6-^{i}Pr$_2$C$_6$H$_3$).[43] All characterization data for these ligands were consistent with the literature.

Synthesis of ligands

L14, $C_{31}H_{23}N_3$. To synthesize **L14**, with R^1 = Ph and R^2 = Ph, 2,6-dibenzoylpyridine (4.0 g, 13.9 mmol), an excess of aniline (4 mL, 4.1 g, 40.0 mmol) and a catalytic amount of *p*-TsOH was refluxed in toluene for 4 days. After cooling to room temperature, the mixture was filtered and the solvent removed *in vacuo* to yield brown/yellow oil which was dissolved in $CHCl_3$ and filtered to remove any remaining *p*-toluenesulfonic acid. Recrystallizing the residue from hot MeOH yielded a yellow crystalline solid, 2.1 g, 33%. ^{1}H NMR spectroscopic analysis at room temperature showed a region of complex resonances between 6.7 and 8.5 ppm, due to restricted rotation of the phenyl rings on the NMR timescale. Resolution of this region *via* high temperature ^{1}H NMR spectroscopy gave the following resonances: ^{1}H NMR (C_6D_6, 80 °C): 8.31 (br s, 2H, *m*-Py-H), 7.93 (br s, 1H, *p*-Py-H), 6.73–7.28 (m, 20H, Ar-*H*). ^{13}C NMR (DMSO-d_6, 115 °C): 166.81, 165.72, 165.47, 156.08, 155.28, 154.38, 153.49, 150.42, 150.21, 137.24, 137.16, 136.73, 134.57, 131.23, 131.14, 129.56, 129.41, 128.60, 128.49, 128.40, 127.40, 127.11, 125.32, 123.64, 123.53, 123.43, 122.67, 120.51, 120.45, 120.26, 120.15. Anal. calcd for $C_{31}H_{23}N_3$: C, 85.10; H, 5.30; N, 9.60. Found: C, 85.24; H, 5.49; N, 9.38. IR (ATR, $\nu_{C=N}$) at 1616 cm^{-1}.

Synthesis of complexes

Many of the [BIMPY]VCl_3 complexes described in this report are found elsewhere in the literature, with **9–14** being novel compounds. Characterization of all compounds is included to maintain consistency throughout. Complexes of the form L_nVCl_3 were prepared using a modified literature procedure, under inert conditions by dissolving the requisite bis(imino) pyridyl ligand and a stoichiometric amount of $VCl_3(THF)_3$ in dichloromethane. The dark red/purple solutions were left to stir overnight. Capricious solubility trends between the complexes were observed as many precipitated as dark solids and could be observed within a few hours, while others remained in solution. In all cases, mixtures were filtered. Any precipitate was washed with DCM and pentane. Filtrates were reduced, and precipitated and washed with pentane before drying *in vacuo*. If impure, the solids were extracted into acetonitrile, or another appropriate solvent, to purify the complex. The

paramagnetic nature of these compounds made characterization by ^{1}H NMR spectroscopy difficult in many cases, but characteristic shifts of diamagnetic protons to paramagnetic regions (~55 and ~−5 ppm) were helpful in confirming complex formation. A consistent bathochromic IR shift of imine bonds characteristic of metallation could also be observed in IR. Evans' method[59] was used to determine the number of unpaired electrons.

$C_{33}H_{43}Cl_3N_3V$, 1. In a glovebox, **L1** (1.00 g, 2.1 mmol) and $VCl_3(THF)_3$ (0.78 g, 2.1 mmol) were combined in a Schlenk tube and dissolved in CH_2Cl_2 (50 mL). The solution was allowed to stir overnight, then filtered and the filtrate reduced to approximately 15 mL. Pentane was added (*ca*. 30 mL) to precipitate a dark solid that was isolated *via* filtration. The dark purple solid was extracted into hot MeCN and any remaining solids were removed *via* filtration. The mixture was reduced *in vacuo*, washed with pentane and dried for several hours. A dark purple solid was obtained (1.12 g, 85%). ^{1}H NMR ($CDCl_3$): 54.76 (6H, N=CCH_3), 8.27 (4H, *m*-Ar-*H*), 5.44 (2H, *p*-Ar-*H*), 4.41 (4H, CH(CH_3)$_2$), 2.79 (24H, CH(CH_3)$_2$), −0.92 (1H, *p*-Py-*H*), −5.81 (2H, *o*-Py-*H*). $\mu_{eff.}$ = 3.3 B.M. (*vs*. 2.83). IR (nujol, cm^{-1}): 1574. Anal. calcd for $C_{33}H_{43}Cl_3N_3V$: C, 62.03; H, 6.78; N, 6.58. Found: C, 62.61; H, 7.01; N, 6.60.

$C_{21}H_{19}Cl_3N_3V$, 2. In a glovebox, **L2** (1.10 g, 3.5 mmol) and $VCl_3(THF)_3$ (1.31 g, 3.5 mmol) were combined in a Schlenk tube and dissolved in CH_2Cl_2 (50 mL). The solution was allowed to stir overnight, then filtered and the filtrate reduced to approximately 15 mL. Pentane was added (*ca*. 30 mL) to precipitate a dark solid that was isolated *via* filtration. The dark brown solid was extracted into hot MeCN and any remaining solids were removed *via* filtration. The mixture was reduced *in vacuo*, washed with pentane and dried for several hours. A dark brown solid was obtained (1.01 g, 73%). ^{1}H NMR (THF-d_8): 83.56 (6H, N=CCH_3), 7.61 (2H, *p*-Ar-*H*), 7.15 (4H, *m*-Ar-*H*), 6.51 (4H, *o*-Ar-*H*), −16.07 (2H, *m*-Py-*H*), −17.09 (1H, *p*-Py-*H*). $\mu_{eff.}$ = 3.3 B.M. (*vs*. 2.83). IR (nujol, cm^{-1}): 1582. Anal. calcd for $C_{21}H_{19}Cl_3N_3V$: C, 53.59; H, 4.07; N, 8.93. Found: C, 53.61; H, 4.01; N, 9.00.

$C_{23}H_{23}Cl_3N_3V$, 3. As for **1**, using **L3** (0.97 g, 2.8 mmol), a stoichiometric amount of $VCl_3(THF)_3$ and CH_2Cl_2 (50 mL). A purple solid was isolated and dried *in vacuo* (1.20 g, 85%). ^{1}H NMR (CD_3CN): 88.99 (6H, N=CCH_3), 12.20 (4H, *o*-Ar-*H*), 4.73 (4H, *m*-Ar-*H*), −1.14 (6H, Ar-CH_3), −16.54 (2H, *m*-Py-*H*), −26.77 (1H, *p*-Py-*H*). $\mu_{eff.}$ = 2.5 B.M. (*vs*. 2.83). IR (nujol, cm^{-1}): 1582. Anal. calcd for $C_{23}H_{23}Cl_3N_3V$: C, 55.39; H, 4.65; N, 8.43. Found: C, 55.25; H, 4.38; Cl, 8.70.

$C_{23}H_{23}Cl_3N_3O_2V$, 4. As for **1**, using **L4** (0.51 g, 1.4 mmol), a stoichiometric amount of $VCl_3(THF)_3$ and CH_2Cl_2 (50 mL). A dark brown solid was recovered and dried *in vacuo* (0.71 g, 95%). ^{1}H NMR (CD_3CN): 92.29 (6H, N=CCH_3), 12.93 (6H, OCH_3), 4.51 (4H, *m*-Ar-*H*), 2.16 (4H, *o*-Ar-*H*), 1.27 (1H, *m*-Py-*H*), −18.06 (1H, *p*-Py-*H*). $\mu_{eff.}$ = 2.9 B.M. (*vs*. 2.83). IR (nujol, cm^{-1}): 1585. Anal. calcd for $C_{23}H_{23}Cl_3N_3O_2V$: C, 52.05; H, 4.37; N, 7.92. Found: C, 52.01; H, 4.35; N, 7.98.

$C_{21}H_{17}Cl_3F_2N_3V$, 5. As for **1** using **L5** (0.53 g, 1.5 mmol), a stoichiometric amount of $VCl_3(THF)_3$ and CH_2Cl_2 (50 mL). A dark brown solid was obtained and dried *in vacuo* (0.48 g, 82%). ^{1}H NMR (CD_3CN): 88.30, 6H, N=CCH_3, 11.86, 4H, *o*-Ar-*H*, 5.29, 4H, *m*-Ar-*H*, −15.82, 2H, *m*-Py-*H*, −25.20, 1H, *p*-Py-*H*. $\mu_{eff.}$ = 2.9 B.M. (*vs*. 2.83). IR (nujol, cm^{-1}): 1582. Anal. calcd for $C_{21}H_{17}Cl_3F_2N_3V$: C, 49.78; H, 3.38; N, 8.29. Found: C, 50.00; H, 3.45; N, 8.08.

$C_{25}H_{27}Cl_3N_3V$, 6. As for **1**, using **L6** (0.60 g, 1.6 mmol), a stoichiometric amount of $VCl_3(THF)_3$ and CH_2Cl_2 (50 mL). The purple solid was dried *in vacuo* (0.68 g, 95%). ^{1}H NMR (CD_3CN): 56.24 (6H, N=CCH_3), 7.27 (4H, *m*-Ar-C*H*), 6.26 (2H, *p*-Ar-C*H*), 4.58 (12H, Ar-CH_3), −1.38 (2H, *m*-Py-*H*), −12.60 (1H, *p*-Py-*H*). $\mu_{eff.}$ = 3.0 B.M. (*vs*. 2.83). IR (nujol, cm^{-1}): 1572. Anal. calcd for $C_{25}H_{27}Cl_3N_3V$: C, 57.00; H, 5.17; N, 7.98. Found: C, 57.05; H, 5.21; N, 7.90.

$C_{29}H_{35}Cl_3N_3V$, 7. As for **1** using **L7** (1.10 g, 2.6 mmol), a stoichiometric amount of $VCl_3(THF)_3$ and CH_2Cl_2 (50 mL). The dark brown solid was dried *in vacuo* (0.92 g, 67%). ^{1}H NMR (CD_3CN): 46.63 (6H, N=CCH_3), 7.50 (*m*-Ar-*H*, 4H), 6.09 (2H, *p*-Ar-*H*), 3.99 (8H, Ar-CH_2CH$_3$), 1.54 (12H, Ar-CH$_2$CH_3), −0.41 (2H, *m*-Py-*H*), −5.57 (1H, *p*-Py-*H*). $\mu_{eff.}$ = 3.1 B.M. (*vs*. 2.83). IR (nujol, cm^{-1}): 1575. Anal. calcd for $C_{29}H_{35}Cl_3N_3V$: C, 59.75; H, 6.05; N, 7.21. Found: C, 59.90; H, 6.16; N, 7.21.

$C_{27}H_{31}Cl_3N_3V$, 8. As for **1**, using **L8** (0.62 g, 1.6 mmol), a stoichiometric amount of $VCl_3(THF)_3$ and CH_2Cl_2 (50 mL). The dark brown solid was dried *in vacuo* (0.60 g, 70%). ^{1}H NMR ($CDCl_3$): 61.34 (6H, N=CCH_3), 8.61 (4H, *m*-Ar-*H*), 7.20 (12H, *o*-Ar-CH_3), 6.4 (6H *p*-Ar-CH_3), −2.3 (2H, *m*-Py-*H*), −10.7 (1H, *p*-Py-*H*). $\mu_{eff.}$ = 2.6 B.M. (*vs*. 2.83). IR (nujol, cm^{-1}): 1577. Anal. calcd for $C_{27}H_{31}Cl_3N_3V$: C, 58.45; H, 5.63; N, 7.57. Found: C, 58.40; H, 5.60; N, 7.62.

$C_{21}H_{31}Cl_3N_3V$, 9. As for **1**, using **L9** (1.06 g, 3.3 mmol), a stoichiometric amount of $VCl_3(THF)_3$ and CH_2Cl_2 (50 mL), yielding a dark purple solid (1.13 g, 85%). ^{1}H NMR ($CDCl_3$): 53.28 (6H, N=CCH_3), 5.32 (8H, *o*-Cy-H_2), 4.84 (8H, *m*-Cy-H_2), 3.07 (4H, *p*-Cy-H_2), 0.91 (1H, *p*-Py-*H*), −4.65 (2H, *m*-Py-*H*). $\mu_{eff.}$ = 3.0 B.M. (*vs*. 2.83). IR (nujol, cm^{-1}): 1578. Anal. calcd for $C_{21}H_{31}Cl_3N_3V$: C, 52.24; H, 6.47; N, 8.70. Found: C, 52.01; H, 6.29; N, 8.88.

$C_{31}H_{39}Cl_3N_3V$, 10. As for **1**, using **L10** (1.01 g, 2.2 mmol), a stoichiometric amount of $VCl_3(THF)_3$ and CH_2Cl_2 (50 mL), yielding a dark purple solid (0.66 g, 67%). ^{1}H NMR (CD_3CN): 8.16 (2H, N=C*H*), 6.88 (4H, *m*-Ar-*H*), 5.44 (2H, *p*-Ar-*H*), 2.97 (4H, CH(CH_3)$_2$), 1.25 (24H, CH(CH_3)$_2$), −5.70 (1H, *p*-Py-*H*), −101.00 (2H, *m*-Py-H). $\mu_{eff.}$ = 2.7 B.M. (*vs*. 2.83) IR (nujol, cm^{-1}): 1570. Anal. calcd for $C_{31}H_{39}Cl_3N_3V$: C, 60.94; H, 6.43; N, 6.88. Found: C, 61.19; H, 6.18; N, 7.02.

$C_{43}H_{47}Cl_3N_3V$, 11. As for **1**, using **L11** (2.12 g, 3.5 mmol), a stoichiometric amount of $VCl_3(THF)_3$ and CH_2Cl_2 (50 mL), yielding a dark purple solid (1.42 g, 58%). ^{1}H NMR ($CDCl_3$): 9.46 (4H, N=C-*o*-Ar-*H*), 8.19 (4H, N=C-*m*-Ar-*H*), 6.27 (2H, N=C-*p*-Ar-*H*), 5.30 (4H, CH(CH_3)$_2$), 4.69 (4H, C=N-*m*-Ar-*H*), 4.35 (C=N-*p*-Ar-*H*), 2.19 (24H, CH(CH_3)$_2$), 0.08 (1H, *p*-Py-*H*), −8.08 (2H, *m*-Py-*H*). $\mu_{eff.}$ = 2.6 B.M. (*vs*. 2.83). IR (nujol, cm^{-1}): 1567. Anal. calcd for $C_{43}H_{47}Cl_3N_3V$: C, 67.67; H, 6.21; N, 5.51. Found: C, 67.45; H, 5.95; N, 5.24.

$C_{35}H_{47}Cl_3N_3V$, 12. As for **1**, using **L12** (0.75 g, 1.5 mmol), a stoichiometric amount of $VCl_3(THF)_3$ and CH_2Cl_2 (50 mL),

yielding a dark purple solid (0.69 g, 70%). ^{1}H NMR (CD_3CN): 32.08 (4H, N=C-CH_2CH$_3$), 8.67 (4H, C=N-*m*-Ar-*H*), 5.44 (2H, C=N-*p*-Ar-*H*), 4.77 (4H, C*H*CH$_3$), 1.21 (6H, N=CCH$_2$C*H*$_3$), 1.02 (24H, ArCHC*H*$_3$), 0.48 (1H, *p*-Py-*H*), −4.19 (2H, *m*-Py-*H*). $\mu_{eff.}$ = 2.4 B.M. (*vs*. 2.83). IR (nujol, cm^{-1}): 1574. Anal. calcd for $C_{35}H_{47}Cl_3N_3V$: C, 63.02; H, 7.10; N, 6.30. Found: C, 63.55; H, 7;45; N, 5.97. Elemental analysis was inaccurate, likely due to decomposition of the sample in transit.

$C_{37}H_{51}Cl_3N_3V$, 13. As for **1**, using **L13** (0.44 g, 0.8 mmol), a stoichiometric amount of $VCl_3(THF)_3$ and CH_2Cl_2 (50 mL), yielding a dark purple solid (0.30 g, 53%). $\mu_{eff.}$ = 2.8 B.M. (*vs*. 2.83). IR (nujol, cm^{-1}): 1565. ^{1}H NMR could not be accurately assigned, due to the complexity of the spectrum. Anal. calcd for $C_{37}H_{51}Cl_3N_3V$: C, 63.93; H, 7.40; N, 6.05. Found: 63.57; H, 7.13; N, 5.83.

$C_{31}H_{23}Cl_3N_3V$, 14. As for **1**, using **L14** (0.78 g, 1.8 mmol), a stoichiometric amount of $VCl_3(THF)_3$ and CH_2Cl_2 (50 mL), yielding a dark purple solid (0.92 g, 89%). ^{1}H NMR (CD_3CN): 11.34 (4H, N=C-*o*-Ar-C*H*), 10.61 (4H, N=C-*m*-Ar-C*H*), 8.79 (2H, N=C-*p*-Ar-C*H*), 5.75 (4H, C=N-*o*-Ar-C*H*), 4.11 (2H, C=N-*p*-Ar-C*H*), 2.10 (C=N-*m*-C*H*), −17.53 (2H, *m*-Py-*H*), −21.43 (1H, *p*-Py-*H*). $\mu_{eff.}$ = 2.6 B.M. (*vs*. 2.83). IR (nujol, cm^{-1}): 1580. Anal. calcd for $C_{31}H_{23}Cl_3N_3V$: C, 62.59; H, 3.90; N, 7.06. Found: C, 62.77; H, 4.12; N, 6.85.

Polymerization experiments

All polymerization experiments were conducted under inert atmosphere. Monomer, initiator and catalyst were loaded into an ampoule or sealed vial along with a magnetic stir-bar with a desired volume of solvent, if required, prior to being placed in a preheated oil bath. After the allotted time, the vessels were run under cold water for 5 minutes to halt the polymerization. Percent conversion was calculated gravimetrically from the mass-to-mass ratio of polymer to starting materials. Molecular weights were obtained relative to polystyrene standards and corrected for low molecular weight VAc.[60]

X-ray crystallography

Crystals were grown by slow evaporation from MeCN or CD_3CN/DCM at room temperature before being coated in Paratone-N oil, mounted using a polyimide MicroMount and frozen in the cold nitrogen stream of the goniometer. A hemisphere of data was collected on a Bruker AXS P4/SMART 1000 diffractometer using ω and φ scans with a scan width of 0.3° and 30 s exposure times with a detector distance of 5 cm. The crystal of **14** was a multiple twin and the orientation matrixes for the three major components were determined, reduced and corrected for absorption. The structure was solved by direct methods and refined by full-matrix least squares on F^2 (SHELXTL) on all data. All non-hydrogen atoms were refined using anisotropic displacement parameters. Hydrogen atoms were found in Fourier difference maps and refined using isotropic displacement parameters. The two structures were deposited in the Cambridge Crystallography Database with numbers CCDC 891101 and 891100 for **12** and **14** respectively.

Acknowledgements

The authors thank the Natural Sciences and Engineering Research Council of Canada, the Canada Foundation for Innovation, the Atlantic Canada Opportunities Agency, the University of Prince Edward Island and the University of Edinburgh for funding.

Notes and references

1 A. Debuigne, R. Poli, C. Jérôme, R. Jérôme and C. Detrembleur, *Prog. Polym. Sci.*, 2009, **34**, 211–239.
2 L. E. N. Allan, M. R. Perry and M. P. Shaver, *Prog. Polym. Sci.*, 2012, **37**, 127–156.
3 F. di Lena and K. Matyjaszewski, *Prog. Polym. Sci.*, 2010, **35**, 959–1021.
4 C. J. Hawker, A. W. Bosman and E. Harth, *Chem. Rev.*, 2001, **101**, 3661–3688.
5 G. Moad, E. Rizzardo and S. H. Thang, *Acc. Chem. Res.*, 2008, **41**, 1133–1142.
6 S. Yamago, *Chem. Rev.*, 2009, **109**, 5051–5068.
7 K. Matyjaszewski, in *Controlled/Living Radical Polymerization: Progress in ATRP, NMP and RAFT*, ed. K. Matyjaszewski, Oxford University Press, ACS, Washington, D.C., 2000.
8 M. Kamigaito, T. Ando and M. Sawamoto, *Chem. Rev.*, 2001, **101**, 3689–3745.
9 K. Matyjaszewski and J. Xia, *Chem. Rev.*, 2001, **101**, 2921–2990.
10 M. Ouchi, T. Terashima and M. Sawamoto, *Acc. Chem. Res.*, 2008, **41**, 1120–1132.
11 K. Matyjaszewski and N. V. Tsarevsky, *Nat. Chem.*, 2009, **1**, 276–288.
12 M. Ouchi, T. Terashima and M. Sawamoto, *Chem. Rev.*, 2009, **109**, 4963–5050.
13 R. Poli, *Eur. J. Inorg. Chem.*, 2011, **2011**, 1513–1530.
14 R. Poli, *Angew. Chem., Int. Ed.*, 2006, **45**, 5058–5070.
15 K. M. Smith, W. S. McNeil and A. S. Abd-El-Aziz, *Macromol. Chem. Phys.*, 2010, **211**, 10–16.
16 M. Hurtgen, C. Detrembleur, C. Jérôme and A. Debuigne, *Polym. Rev.*, 2011, **51**, 188–213.
17 H. Kaneyoshi and K. Matyjaszewski, *Macromolecules*, 2005, **38**, 8163–8169.
18 M. Hurtgen, A. Debuigne, C. Jérôme and C. Detrembleur, *Macromolecules*, 2010, **43**, 886–894.
19 C. Detrembleur, D.-L. Versace, Y. Piette, M. Hurtgen, C. Jérôme, J. Lalevee and A. Debuigne, *Polym. Chem.*, 2012, **3**, 1856–1866.
20 A. Debuigne, J. Warnant, R. Jérôme, I. Voets, A. de Keizer, M. A. Cohen Stuart and C. Detrembleur, *Macromolecules*, 2008, **41**, 2353–2360.
21 A. Debuigne, C. Michaux, C. Jérôme, R. Jérôme, R. Poli and C. Detrembleur, *Chem.–Eur. J.*, 2008, **14**, 7623–7637.
22 C. Detrembleur, A. Debuigne, O. Altintas, M. Conradi, E. H. H. Wong, C. Jérôme, C. Barner-Kowollik and T. Junkers, *Polym. Chem.*, 2012, **3**, 135–147.

23 M. R. Buchmeiser and M. G. Marino, *Macromol. Mater. Eng.*, 2012, **297**, 894–901.
24 A. Debuigne, J. R. Caille, C. Detrembleur and R. Jérôme, *Angew. Chem., Int. Ed.*, 2005, **44**, 3439–3442.
25 A. Debuigne, J. R. Caille and R. Jérôme, *Angew. Chem., Int. Ed.*, 2005, **44**, 1101–1104.
26 C. Detrembleur, A. Debuigne, R. Bryaskova, B. Charleux and R. Jérôme, *Macromol. Rapid Commun.*, 2006, **27**, 37–41.
27 V. Sciannamea, A. Debuigne, Y. Piette, R. Jérôme and C. Detrembleur, *Chem. Commun.*, 2006, 4180–4182.
28 S. Maria, H. Kaneyoshi, K. Matyjaszewski and R. Poli, *Chem.–Eur. J.*, 2007, **13**, 2480–2492.
29 A. Debuigne, Y. Champouret, R. Jérôme, R. Poli and C. Detrembleur, *Chem.–Eur. J.*, 2008, **14**, 4046–4059.
30 D. N. Bunck, G. P. Sorenson and M. K. Mahanthappa, *J. Polym. Sci., Part A: Polym. Chem.*, 2011, **49**, 242–249.
31 R. Bryaskova, C. Detrembleur, A. Debuigne and R. Jérôme, *Macromolecules*, 2006, **39**, 8263–8268.
32 H. Kaneyoshi and K. Matyjaszewski, *Macromolecules*, 2006, **39**, 2757–2763.
33 K. S. S. Kumar, Y. Gnanou, Y. Champouret, J. C. Daran and R. Poli, *Chem.–Eur. J.*, 2009, **15**, 4874–4885.
34 K. S. S. Kumar, Y. Li, Y. Gnanou, U. Baisch, Y. Champouret, R. Poli, K. C. D. Robson and W. S. McNeil, *Chem.–Asian J.*, 2009, **4**, 1257–1265.
35 V. C. Gibson, C. Redshaw and G. A. Solan, *Chem. Rev.*, 2007, **107**, 1745–1776.
36 G. J. P. Britovsek, M. Bruce, V. C. Gibson, B. S. Kimberley, P. J. Maddox, S. Mastroianni, S. J. McTavish, C. Redshaw, G. A. Solan, S. Stromberg, A. J. P. White and D. J. Williams, *J. Am. Chem. Soc.*, 1999, **121**, 8728–8740.
37 B. Cetinkaya, E. Cetinkaya, M. Brookhart and P. S. White, *J. Mol. Catal. A: Chem.*, 1999, **142**, 101–112.
38 R. Schmidt, M. B. Welch, R. D. Knudsen, S. Gottfried and H. G. Alt, *J. Mol. Catal. A: Chem.*, 2004, **222**, 9–15.
39 R. Schmidt, M. B. Welch, R. D. Knudsen, S. Gottfried and H. G. Alt, *J. Mol. Catal. A: Chem.*, 2004, **222**, 17–25.
40 R. Schmidt, P. K. Das, M. B. Welch and R. D. Knudsen, *J. Mol. Catal. A: Chem.*, 2004, **222**, 27–45.
41 M. E. Bluhm, C. Folli and M. Doring, *J. Mol. Catal. A: Chem.*, 2004, **212**, 13–18.
42 C. Bianchini, G. Giambastiani, L. Luconi and A. Meli, *Coord. Chem. Rev.*, 2006, **254**, 431–455.
43 S. McTavish, G. J. P. Britovsek, T. M. Smit, V. C. Gibson, A. J. P. White and D. J. Williams, *J. Mol. Catal. A: Chem.*, 2007, **261**, 293–300.
44 O. Dayan and B. Cetinkaya, *J. Mol. Catal. A: Chem.*, 2007, **271**, 134–141.
45 L.-H. Guo, H.-Y. Gao, L. Zhang, F.-M. Zhu and Q. Wu, *Organometallics*, 2010, **29**, 2118–2125.
46 D. Sieh, M. Schlimm, L. Andernach, F. Angersbach, S. Nückel, J. Schöffel, N. Šušnjar and P. Burger, *Eur. J. Inorg. Chem.*, 2012, **2012**, 444–462.
47 T. M. Smit, A. K. Tomov, G. J. P. Britovsek, V. C. Gibson, A. J. P. White and D. J. Williams, *Catal. Sci. Technol.*, 2012, **2**, 643–655.
48 J. R. V. Lang, C. E. Denner and H. G. Alt, *J. Mol. Catal. A: Chem.*, 2010, **322**, 45–49.
49 N. V. Semikolenova, V. A. Zakharov, L. G. Echevskaja, M. A. Matsko, K. P. Bryliakov and E. P. Talsi, *Catal. Today*, 2009, **144**, 334–340.
50 J. Romero, F. Carrillo-Hermosilla, A. Antinolo and A. Otero, *J. Mol. Catal. A: Chem.*, 2009, **304**, 180–186.
51 M. P. Shaver, M. E. Hanhan and M. R. Jones, *Chem. Commun.*, 2010, **46**, 2127–2129.
52 L. E. N. Allan, E. D. Cross, T. W. Francis-Pranger, M. E. Hanhan, M. R. Jones, J. K. Pearson, M. R. Perry, T. Storr and M. P. Shaver, *Macromolecules*, 2011, **44**, 4072–4081.
53 D. Reardon, F. Conan, S. Gambarotta, G. Yap and Q. Wang, *J. Am. Chem. Soc.*, 1999, **121**, 9318–9325.
54 R.-P. Nzé, O. Colombani and E. Nicol, *J. Polym. Sci., Part A: Polym. Chem.*, 2012, **50**, 4046–4054.
55 C. Barner-Kowollik and G. T. Russell, *Prog. Polym. Sci.*, 2009, **34**, 1211–1259.
56 R.-Q. Fan, D.-S. Zhu, Y. Mu, G.-H. Li, Y.-L. Yang, Q. Su and S.-H. Feng, *Eur. J. Inorg. Chem.*, 2004, 4891–4897.
57 M. A. Esteruelas, A. M. Lopez, L. Mendez, M. Olivan and E. Onate, *Organometallics*, 2003, **22**, 395–406.
58 T. Jurca, K. Dawson, I. Mallov, T. Burchell, G. P. A. Yap and D. S. Richeson, *Dalton Trans.*, 2010, **39**, 1266–1272.
59 D. F. Evans, *J. Chem. Soc.*, 1959, 2003–2005.
60 T. Gruendling, T. Junkers, M. Guilhaus and C. Barner-Kowollik, *Macromol. Chem. Phys.*, 2010, **211**, 520–528.